Boron-Mediated Growth of Long Helicity-Selected Carbon Nanotubes

X. Blase,[1,3] J.-C. Charlier,[2,3] A. De Vita,[3,4] and R. Car[3,5,*]

[1]*Université Claude Bernard-Lyon I and CNRS, Département de Physique des Matériaux (UMR 5586), 43, boulevard du 11 novembre 1918, 69622 Villeurbanne Cédex, France*

[2]*Unité de Physico-Chimie et de Physique des Matériaux, Université Catholique de Louvain, Place Croix du Sud 1, B-1348, Louvain-la-Neuve, Belgium*

[3]*Institut Romand de Recherche Numérique en Physique des Matériaux (IRRMA), INR-Ecublens, CH-1015 Lausanne, Switzerland*

[4]*INFM and Dipartimento di Ingegneria dei Materiali, Università di Trieste, via A. Valerio 2, 34127 Trieste, Italy*

[5]*Département de Physique de la Matière Condensée, Université de Genève, 24 quai Ernest-Ansermet, CH1211 Genève 4, Switzerland*

Ph. Redlich,[6] M. Terrones,[7,8] W. K. Hsu,[7] H. Terrones,[8] D. L. Carroll,[9] and P. M. Ajayan[10]

[6]*Max-Planck-Institut für Metallforschung, Seestrasse 92, D-70174, Germany*

[7]*School of Chemistry, Physics and Environmental Science, University of Sussex, Brighton BN1 9QJ, United Kingdom*

[8]*Instituto de Física, UNAM, Apartado Postal 1-1010, 76000 Querétaro, México*

[9]*Department of Physics and Astronomy, Clemson University, Clemson, South Carolina 29634*

[10]*Department of Material Sciences and Engineering, Rensselaer Polytechnic Institute, Troy, New York 12180-3590*

(Received 30 April 1999)

We investigate the growth of B-doped carbon nanotubes combining experimental and theoretical techniques. Electron microscopy observations and electron diffraction patterns reveal that B doping considerably increases the length of carbon tubes and leads to a remarkable preferred zigzag chirality. These findings are corroborated by first-principles static and dynamical simulations which indicate that, in the zigzag geometry, B atoms act as a surfactant during growth, preventing tube closure. This mechanism does not extend to armchair tubes, suggesting a helicity selection during growth.

PACS numbers: 71.20.Tx, 68.65.+g

Since their discovery, many experimental and theoretical studies have focused on identifying the parameters which determine the production yields and the geometry of carbon nanotubes (CN) [1]. Outstanding results have been achieved in producing well calibrated pure CNs [2]. Recent experiments show that boron doping [3–7] not only changes the electronic properties of the host CN [5,6] but also significantly improves their crystallinity and aspect ratio [4]. It is further known that B doping significantly increases the stiffness of carbon fibers [8] and plays an important role in the resistance to oxidation of graphitic systems [9]. These results suggest that B doping might be a good way to produce long and well graphitized carbon nanotubes with interesting mechanical and electronic properties. While the effect of doping on the nanotube electronic properties has already been studied [5], the mechanisms driving the structural changes observed under doping are as yet unclear.

In this work, we present a joint theoretical and experimental study of the topology and growth mechanisms of B-doped carbon nanotubes (BDCN). We first report on the synthesis of such tubes and on the experimental study of their structural properties. We show that the incorporation during growth of a small quantity of B atoms ($\leq 2\%$) induces dramatic changes in the host CN morphology. In particular, high resolution transmission electron microscopy (HRTEM) and selected area electron diffraction (SAED) data reveal an important length increase and, for the first time, a helicity selection of the produced BDCNs. We rationalize these findings on the basis of the results of first-principles molecular dynamics (MD) simulations [10], performed within the framework of density functional theory (DFT) [11].

The samples are prepared using an arc-discharge dc generator normally employed for fullerene production. The anodes are graphite rods drilled and filled with B or BN powders. The cathodes are made of pure graphite. The chamber is first purged twice and then filled with a nitrogen or helium gas at 200–500 Torr pressure. The arcing conditions vary from 25 V, 80 A to 40 V, 150 A. A $\sim$ 1 mm gap is maintained between the electrodes. The produced inner core cathode deposit is removed and analyzed by HRTEM, SAED, and energy electron loss spectroscopy (EELS). More details about the experimental setup can be found in Ref. [4]. TEM images from the cathode deposit show that all samples contain remarkably long multiwall nanotubes (MWNTs) (up to 100 μm), and small amounts of polyhedral particles (the nanotube/particle ratio is 8:2). Small B_4C-like microcrystals are also present, as identified by x-ray diffraction analysis. Another remarkable observation is that in the long BDCNs, *the zigzag or near-zigzag chirality is preferred*, as revealed by the SAED patterns of individual BDCNs [12]. A statistical analysis of the *hk*0 reflections based on 20 BDCNs (see Fig. 1b) shows that the distribution is strongly enhanced around $\alpha = 30°$ which is characteristic of the zigzag helicity. On the contrary,

 0031-9007/99/83(24)/5078(4)$15.00

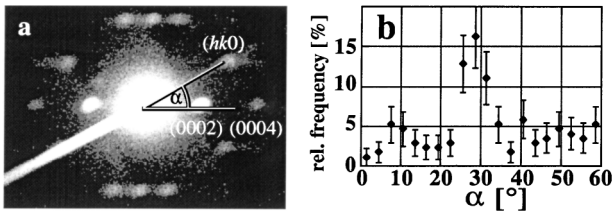

FIG. 1. Electron diffraction patterns for B-doped carbon nanotubes. In (a), a typical diffraction pattern of an individual tube generated at low arc current and high B concentration. In (b), statistical analysis of the angular distribution of *hk*0 reflections. The frequency values are normalized to the total number of reflections analyzed; error bars correspond to the standard deviations assuming Poisson statistics. The angle α [see (a)] is measured with respect to the direction of the 0002 reflections, i.e., the direction perpendicular to the tube axis (error: ruler precision; $\pm 2°$).

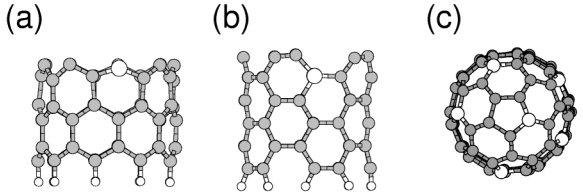

FIG. 2. Symbolic ball-and-stick representation of various B-doped carbon nanotube lips. In (a) and (b), C(9,0) and C(5,5) edges, respectively, are represented. In (c), the B-doped hemi-C_{60} caped C(5,5) nanotube used for the MD run is seen from the top.

chiralities corresponding to the armchair configuration ($\alpha = 0°, 60°$) are rarely observed and other helical arrangements are never dominating. We emphasize that the preferential zigzag helicity is also found in thick BDCNs with typically more than 20 layers. This is in significant contrast with the case of pure carbon nanotubes, where, as reported in Ref. [13], a $\sim 3°$ change of chirality is observed every 4–5 graphitic shells leading to a "continuous" ring distribution of the intensity of the *hk*0 reflections.

EELS analysis allows one to study the concentration of B atoms in the nanotube. This is found to depend on the applied current and B concentration. At high current ($\geq$100 A) and low B concentration in the anode filling (at C/B or C/BN ratios of 2/1 or 5/1 by weight, respectively), B can be detected only at the tip of the nanotube. In this case, the tube body is found to be made of pure carbon (B content is below the detection limit of about 1 at. %). Ill-formed tips, occasionally opened or presenting negative curvature (toroidal shape) are observed. As discussed further below, these results suggest that B atoms preferentially remain at the tip of the growing nanotube. At lower current (70–100 mA) and higher B concentration (at C/B or C/BN ratios of 1/1 or 1/3, respectively), the B concentration increases in the body of the produced nanotubes (up to 5%) but, surprisingly enough, does not increase at the tip. The B-doped nanotubes display well graphitized tips, with fewer defects. No structural alteration was observed using N_2 instead of He in the reaction chamber.

To understand these results, we now compare the energetics and the dynamics of B-doped zigzag and armchair nanotubes. We perform first-principles calculations within the local density approximation [14] to DFT. Technical details and run parameters are as in Ref. [15], where the growth of pure C and BN nanotubes has been studied. We first study the relative energies of structures obtained by substituting a C atom with a B atom at different locations of the open end of a (9,0) zigzag [16] nanotube (see Fig. 2a). After atomic relaxation, we find that B atoms preferentially substitute the two-coordinated topmost C atoms at the tube end. Substitutional B atoms located one, two, and three bonds away from this location into the tube body are found to be less stable by 0.9, 0.4, and 1.5 eV, respectively. Clearly, the stabilization of B atoms at the zigzag edge is due to the removal of dangling bonds at the two-coordinated atomic sites. Similar results are obtained for a graphitic zigzag edge (see Fig. 3), indicating that the energy ordering is independent of the curvature and thus of the radius of the nanotube. These results suggest that B atoms will preferentially remain on the "lip" of the nanotubes, thus acting as surfactant during the growth [17].

We now address the role of surfactant B atoms in the dynamical behavior of zigzag nanotubes at synthesis temperature by means of finite temperature first-principles MD. As a test case, we consider a C(9,0) nanotube in an open-end configuration terminated by a complete ring of two-coordinated B atoms [18]. Starting from this "ideal" cleaved B-terminated geometry, we gradually raise the temperature up to 2500 K, which is typical of the experimental synthesis conditions. At a relatively low temperature ($\sim$500 K), the only observed phenomenon is that B atoms transiently dimerize (Fig. 4a). At $\sim$2500 K, B trimers are created, followed by the appearance of B-B-B-C-C and C pentagons at the tip of the nanotube (Fig. 4b). The formation of pentagons causes a substantial bending inwards of the edge structure, rapidly leading to partial

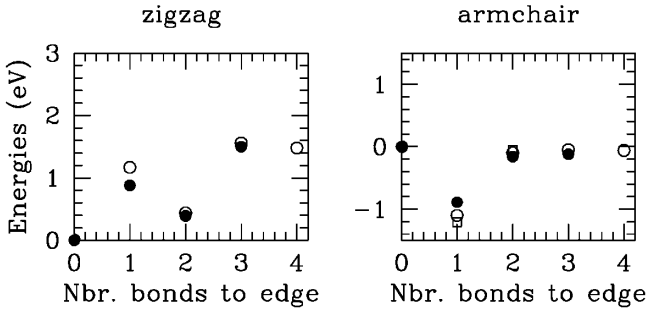

FIG. 3. Substitutional energy for B atoms at various sites in the zigzag and armchair cases. The reference of energy is taken to be the "edge" site. In both cases, filled and empty circles indicate the results for, respectively, the model nanotubular systems represented in Figs. 2a and 2b and a planar graphene sheet edge. The empty squares indicate calculations on a C_{24} flake presenting an armchair rim.

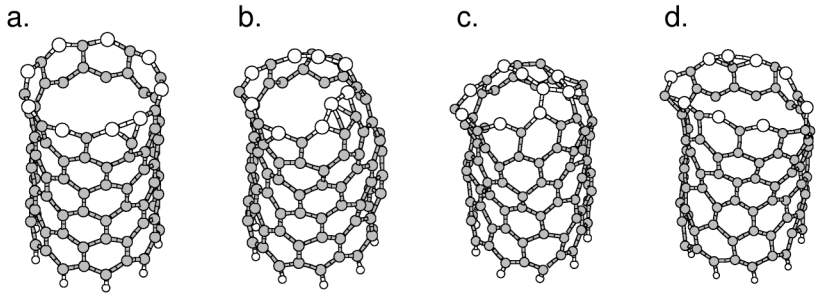

FIG. 4. Symbolic ball-and-stick representation of a B-doped C(9,0) nanotube. In (a), the ground state geometry at $T = 0$ K is represented. In (b), (c), and (d) three different snapshots for the nanotube at 2500 K are given. Snapshot (d) represents the final configuration reached by the system at the end of the MD run.

closure through the creation of an atomic "bridge" across the end of the nanotube (Fig. 4c). This is similar to what was observed in the case of single-wall carbon nanotubes (SWNTs) [15]. However, in contrast with the pure CN case where the bridging quickly led to tip closure into a defected graphitic dome, here the B-B bonds easily break, and the tip structure of the BDCN eventually reopens. The reopened structure (Fig. 4d) is identical to the one in Fig. 4b except for the transfer of one B atom on the opposite side of the tube edge. In contrast with the CN case, the presence of a C pentagon (front right of Figs. 4b–4d) is not sufficient to drive the system to full tip closure. Further, we verify that C pentagons located at the edge of an open-ended nanotube reopen spontaneously to form a hexagon upon arrival of a C atom from the vapor phase [19]. This indicates that a C pentagon which does not succeed in closing the tube tip is short lived at the growing edge.

It appears therefore that B atoms located at the top of growing zigzag CNs can act against tube closure. This would explain the increased length of zigzag B-doped carbon nanotubes. We note that while the present simulations were performed on a SWNT, similar conclusions also apply to the case of MWNTs. Since it opposes the closure of each individual shell, B doping is expected to favor the growth of long MW tubes. The ability of growing long tubes is by itself an important result, given the importance attached to the production of long ballistic one-dimensional nanoconductors [20], or of large aspect ratio fibers for composite materials [21]. It is well known, however, that the electronic properties of a nanotube depend strongly on the tube helicity. Therefore, a further important development in the nanotube production techniques would be the ability of selectively growing long structures with a given helicity.

We now turn to the helicity selection revealed by the experiments. The same kind of mechanism discussed above for a zigzag tube may *a priori* apply to armchair nanotubes. We therefore perform the same type of analysis for armchair BDCNs. In contrast with the zigzag case, we find that the preferred substitutional site is not on the lip of the open nanotube but is located instead one bond away from the edge (see Figs. 2b and 3). In this most stable site, the B atom is threefold coordinated, which makes it much less mobile (and, thus, less likely to act as a surfactant) than it would be as an edge atom. In the case of a C(5,5) nanotube, this configuration is found to be 0.9 eV more stable than the B-C dangling-dimer configuration and 0.75 eV more stable than a configuration in which the B atom is three bonds away from the lip. Once more, similar results (Fig. 3) are obtained at the armchair edge of a graphitic sheet and for a C_{24} flake with a rim presenting dangling dimers only. We note that while dangling C_2 dimers can be stabilized by dangling bond pairing, the formation of an "unbalanced" B-C pair seems to significantly reduce the efficiency of this hybridization, explaining therefore the relative instability of the dangling BC dimer. Since we are left with no mechanism to place B mobile atoms at the very edge of the growing structure, it seems difficult at this stage to generalize to the armchair case the results obtained earlier for the zigzag tube. In a further simulation, starting from a C(5,5) tube closed by the B-doped hemi-C_{60} represented in Fig. 2c, we did not observe the cap reopening during 10 ps of simulations at 3000 K [22].

Comparing this simulation with the one described above in the case of the zigzag tube, it seems likely that maximizing the number of B-B bonds upon attempted closure is crucial for observing the "reopening" of the tip. Since in the armchair case B atoms tend to "sink" into the graphitic network, B-B bonds will form much less frequently (if at all) and will thus not be available to play the catalytic role observed in the zigzag case. This can explain why B atoms, acting as surfactant, can selectively catalyze the growth of long zigzag nanotubes. We note, however, that the present simulations do not rule out the growth of MWNTs of "standard" length with chiral or armchair helicities.

In conclusion, we have presented experimental evidence that B doping of carbon nanotubes catalyzes the growth of long ($\sim 5-100$ μm) and well graphitized nanotubes. These results are corroborated by first-principles static calculations and dynamical simulations which support a model of surfactant B atoms catalyzing the growth

of long nanotubes. The model applies only to the zigzag tube geometry, implying that this nonchiral geometry should be favored in B-doped nanotubes with a large aspect ratio. This is consistent with the helicity preference revealed by the experimental ED patterns.

This work was partially supported by the Swiss NSF and the DFG Contract No. Ru342/11-1. We also thank the Royal Society (M. T.), the EPSRC (W. K. H.), CONACYT-Mexico (H. T.), DGAPA-UNAM IN 107-296 (H. T.), and TWAS No. 97-178 RG/PHYS/LA (H. T.) for financial support.

*New permanent address: Department of Chemistry and Princeton Materials Institute, Princeton University, Washington Road and William Street, Princeton, NJ 08544-1009.

[1] S. Iijima, Nature (London) **354**, 56 (1991).
[2] T. W. Ebbesen, Phys. Today **49**, No. 6, 26 (1996); A. Thess *et al.,* Science **273**, 483 (1996).
[3] O. Stephan *et al.,* Science **266**, 1683 (1994); Z. Weng-Sieh *et al.,* Phys. Rev. B **51**, 11 229 (1995).
[4] Ph. Redlich *et al.,* Chem. Phys. Lett. **260**, 465 (1996).
[5] D. L. Carroll *et al.,* Phys. Rev. Lett. **81**, 2332 (1998); J.-Y. Yi and J. Bernholc, Phys. Rev. B **47**, 1708 (1993).
[6] M. Terrones *et al.,* Appl. Phys. A **66**, 307 (1998).
[7] D. Goldberg, Y. Bando, K. Kurashima, and T. Sasaki, Appl. Phys. Lett. **72**, 2108 (1998); W. Q. Han, Y. Bando, K. Kurashima, and T. Sato, Chem. Phys. Lett. **299**, 368 (1999).
[8] A. Agarwal *et al.,* J. Mater. Sci. **21**, 3455 (1986).
[9] X. Ma *et al.,* Carbon **35**, 1517 (1997); L. R. Radovic, M. Karra, K. Skokova, and P. A. Thrower, Carbon **36**, 1841 (1998), and references therein.
[10] R. Car and M. Parrinello, Phys. Rev. Lett. **55**, 2471 (1985).
[11] P. Hohenberg and W. Kohn, Phys. Rev. **136**, B864 (1964); W. Kohn and L. J. Sham, Phys. Rev. **140**, A1133 (1965).
[12] A. A. Lucas, V. Bruyninckx, and P. Lambin, Europhys. Lett. **35**, 355 (1996); P. Lambin and A. A. Lucas, Phys. Rev. B **56**, 3571 (1997).
[13] M. Liu and J. M. Cowley, Carbon **32** (1994).
[14] D. M. Ceperley and B. J. Alder, Phys. Rev. Lett. **45**, 566 (1980).
[15] J.-C. Charlier, A. De Vita, X. Blase, and R. Car, Science **275**, 646 (1997); X. Blase, A. De Vita, J.-C. Charlier, and R. Car, Phys. Rev. Lett. **80**, 1666 (1998).
[16] With standard notations, $(n, 0)$ and (n, n) nanotubes are called, respectively, zigzag and armchair; see N. Hamada, S. Sawada, and A. Oshiyama, Phys. Rev. Lett. **68**, 1579 (1992).
[17] Starting from an ideal graphitic "zigzag edge," and not allowing for structural relaxation upon B substitution, the second-to-edge site local minimum disappears. This indicates that the relative stability of this site cannot be inferred from considerations based only on the electronic stability of different bond topologies and that one needs to account for the gain in elastic energy upon relaxation of the network around the B atom in each configuration (the B-C bond length is found to be 1.42 Å at the edge and 1.48 Å in the bulk).
[18] The studied nanotube contains 117 atoms, including 9 B and 9 H atoms. The H atoms are used to passivate the nanotube end opposite to the "growing lip." They are maintained fixed during the simulation. The total simulation time is of $\sim$10 ps.
[19] Starting from the configuration of Fig. 4d, we have added an extra C atom, located 2 Å away from the middle of the "B-connected" pentagon edge in a direction perpendicular to the tube axis. Upon structural relaxation at $T = 0$ K, the adatom moves towards the pentagon edge which spontaneously reopens (without any barrier) to accommodate the incoming atom.
[20] S. J. Tans *et al.,* Nature (London) **386**, 474 (1997); C. T. White and T. N. Todorov, Nature (London) **393**, 240 (1998).
[21] B. I. Yakobson and R. E. Smalley, Am. Sci. **85**, 324 (1997).
[22] The initial cap was prepared assuming closure without formation of B-B bonds. We note such a tip exhibits a rather large $\sim$20% doping (6 B atoms out of 30 C atoms), much larger than what is measured for the body of the nanotube. This implies that the effect of isolated B atoms on the electronic properties (see Ref. [5]) of the nanotube body or cap is not sufficient to enhance the growth of carbon nanotubes.